Accepted Version
Journal of American Ceramic society

Synthesis and Morphological Analysis of Titanium Carbide Nanopowder

D. Sarkar[1#], M. C. Chu[1*], S. J.Cho[1], Y.I. Kim[1] and B.Basu[2†]

[1]Korea Research Institute of Standards and Science,
Yusong-Gu, Daejeon 305-340, Republic of Korea

[2]Department of Materials and Metallurgical Engineering,
Indian Institute of Technology, Kanpur, UP-208016, India

Abstract

One of the major challenges in the development of nanostructured/ultrafine non-oxide ceramics is the synthesis of non-agglomerated nanosized ceramic powders. Here, we investigate carbothermal reduction to obtain spherical titanium carbide (TiC) nanoparticles smaller than 100 nm in diameter. Using a combination of characterization techniques, it has been confirmed that optimum thermal reduction conditions include a temperature of 1350^{o}C with 1 hour holding in an argon atmosphere. A three-parameter Weibull distribution function provides a satisfactory fit for the size distribution of the synthesized TiC nanoparticles. Varying the synthesis time at 1350^{o}C revealed the particle coarsening exponent 'n' to be 2.9 and that particle shapes change from spherical at 1 hour to more faceted at longer holding times of 4 hours.

Key Words: TiO_2, TiC, Nanoparticles, Size Distribution

Faculty of Dept. of Ceramic Engg, National Institute of Technology, Rourkela, India (Email:dsarkar@nitrkl.ac.in)
*Corresponding Author: chumin@kriss.re.kr Tel: 82-42-868-5694, Fax: 82-42-868-5032
† Member of American Ceramic Society

1. Introduction

Bulk nanoceramic materials, having grain sizes typically smaller than 100 nm, possess appealing mechanical, physical, and tribological properties[1]. They have therefore been the subject of significant research activity in recent years. One of the major challenges in the research on bulk nanoceramics and nanoceramic composites is the synthesis of nanosized ceramic powders. While the synthesis of nanosized *oxide* powders has been reported, such efforts in the case of *non*-oxide ceramics are not widespread. In this context, we have carried out a research program to develop nanosized TiC.

Titanium Carbide (TiC) has been successfully integrated into structural components, including magnetic recording heads, transparent optical materials, and composite reinforcing materials[1, 2]. TiC can be prepared through several methods. One such method is via common carbothermal reduction of titanium dioxide (TiO_2) powder using carbon[3-5]. Other methods use polymeric precursors based on either titanium alkoxides or other organic compounds[6-8]. Another alternative method is through the direct reaction of Ti and carbon[9]. Gas phase reactions of $TiCl_4$ and hydrocarbons are a relatively new approach to synthesizing TiC[10]. In addition, self-propagating high-temperature synthesis (SHS), Mg-thermal reduction[11, 12], gas-phase laser-induced reactions[13], mechanical milling[14], and laser chemical vapor deposition (LCVD)[15] are also well established techniques for preparing titanium carbide powders. The most popular amongst these methods are the high-energy mechano-chemical and carbothermal reduction (with mineralizer) techniques[10, 16]. Recently, Woo et al. successfully synthesized pure TiC nanoparticles from TiO_2 and carbon resin without any addition of mineralizer[17]. A processing temperature of 1500 ^oC was required for the reduction of 20-30 nm TiO_2 nanoparticles into 80 nm (average size) TiC nanoparticles. Razavi et al. demonstrated that the temperature for the synthesis of TiC can also be reduced by increasing the milling time of both the Ti chips and

carbon black precursors[18]. Feng et al. developed a low temperature (500 ^{o}C) direct chemical synthesis process using $TiCl_4$ and CaC_2. The as-synthesized TiC nanoparticles were 40nm in size and small amount of free carbon as impurity[19]. Gotoh et al. reported the TiC nanoparticle formation mechanism via carbothermal reduction of 5 nm TiO_2 sol and methyl cellulose (MC). Interestingly, the reduction temperature was lower compared with that of conventional reduction techniques[20]. Here, we propose a new additive-free synthesis technique for the preparation of spherical and pure TiC nanoparticles using nano rutile (prepared in-house) and an amorphous carbon powder mixture. The sizes of the obtained TiC particles were evaluated and quantified using Weibull distribution fit parameters.

2. Experimental Procedure

2.1. Powder Preparation

Prior to carbothermal reduction, we prepared a nano rutile powder in-house; details can be found elsewhere[21]. Briefly, titanium tetrachloride, $TiCl_4$, (Junsei, Japan) liquid was used as the starting precursor for the synthesis of TiO_2. Initially, an ethanol (C_2H_5OH) solvent was slowly added until the entire solution became a dark yellowish viscous liquid. Subsequently, ice-cold water was slowly added to the mixture and stirred continuously until a clear solution was obtained. It was then kept at 60 ^{o}C for 4 hours at which time white rutile nano-particles precipitated. The filtrate residue was then washed with hot water to remove any excess chloride ions, and it was then dried at 60 ^{o}C for 4 hours. The dried powder was mixed with carbon black (Goldstar Cable, Korea) and acetone in a high-density polyethylene (Nalgene) jar. The powdered mixture was ball-milled for 2 hours through 3Y-TZP grinding media. The dry black powder mixture was then placed in an alumina crucible and finally positioned within the graphite chamber of a brazing furnace. Thermal treatment was carried out in argon gas at atmospheric

pressure. Prior to heat treatment, pyrolysis behavior of the powder mixture was studied through DTA-TG up to 1400 ^{o}C at a heating rate of 10^{o}C per minute in an Ar gas flow. In order to identify the formation of intermediate phases, the precursor mixture was heat treated at 1200 ^{o}C for 1 hour. Finally, the powdered mixture (TiO_2-C) was calcined at 1350 ^{o}C for 1, 2, and 4 hours.

2.2. Powder Characterization

Phase identification of the as-obtained powders was carried out using x-ray diffraction (Rigaku, XRD) with Cu-α radiation. The voltage and current settings were 40 kV and 40 mA, respectively. XRD patterns of the as-synthesis TiO_2 and TiC nano powders were taken in 0.02° steps from 20^{o} to 145^{o}. The particle size and residual strain of the synthesized TiC nanoparticles was calculated using the Williamson–Hall equation[22]:

$$b\cos\theta = \frac{\lambda}{d} + 2\eta\sin\theta\,, \quad \text{..... (1)}$$

where b is full width (radians) of the peak at half intensity (FWHM), θ is the position of peak obtained from the XRD pattern, λ is the x-ray wavelength (1.54056 ´), η is the powder microstrain, and d is the average crystallite size. The FWHM was modified as $b = (b^2_{meas} - b^2_{equip})^{1/2}$, where b_{meas} and b_{equip} are the measured FWHM and FWHM due to instrumental broadening, respectively. A commercial 2 μm TiC powder (CERAC, USA) was used in this study to obtain standard FWHM values. The particle sizes of the as-synthesized TiO_2 and TiC powders were characterized through transmission electron microscope (TEM, TECNAI-G2, FEI). X-ray fluorescence (XRF, WDXRF 9800 model, Netherlands) was employed to determine the elemental analysis of TiC nanopowders, both at intermediate and final stages. The particle size distributions were measured with a scanning mobility particle size (SMPS, GRIMM, Germany) instrument. Here, the collected particles were electrically charged with an AM241 neutralizer,

detected with a differential mobility analyzer (DMA), and subsequently counted with a concentration particle counter (CPC). Prior to estimation of these size distributions, the TiC particles were dispersed using a 1 wt% polyacrylic acid (PAA) in water.

3. **Results and Discussion**

A first step towards the production of TiC nanoparticles was the synthesis of TiO_2 precursor materials. As described in the previous section, titania precursor was produced and TEM was carried out. The bright field TEM image of the as-synthesized TiO_2 particles is provided in Fig. 1. The selected area diffraction pattern analysis indicated the as-synthesized TiO_2 to be in the rutile phase. In Fig. 1a, a needle-like irregular structure of the nanosized rutile powder is evident. The rutile agglomerates consisted of 5 nm needle-like TiO_2 clusters (Fig. 1b). This specific shape can be attributed to the high $TiCl_4$ concentration in water, for the most part. From the synthesis point of view, a high concentration of $TiCl_4$ initiates rapid hydrolysis and TiO_2 phase formation proceeds by the rearrangement of a TiO_6 octahedral network through vertex sharing. As a result, elongated rutile crystal was produced preferentially. The hydrolysis of $TiCl_4$ reduces the number of OH ligands. This suppresses edge-shared bonding and enhances corner-shared bonding—non-spherical oval-shaped TiO_2 nanoparticle is promoted [23]. From the first principles analysis for the total energy calculation, the vertex (111) plane of the rutile phase has a higher surface energy than that of the edge (110) plane[24]. Such anisotropies encourage the formation of head-to-tail agglomeration, resulting in needle-like secondary particles.

In order to understand the heating induced reactions/dissociation, DTA-TG analysis on TiO_2-C powder mixture was performed in argon atmosphere at a heating rate of 10 ^oC per minute (Fig. 2). The pyrolysis process illustrates a significant endothermic peak at 1114 ^oC that ranges from 800 ^oC to 1380 ^oC. In addition, the thermo gravimetric (TG) curve of the powder mixture

shows a gradual weight loss of about 8% in the temperature range 600–915 ^{o}C and a sharp weight loss of about 34% in the temperature range 915–1189 ^{o}C. Further weight loss of about 6% occurs up to a temperature of 1378 ^{o}C. The first-step weight loss and endothermic peak are presumed to be due to the rapid formation of an unstable oxygen deficient T_nO_{2n-1} (one of the Magneli phases, n = 4 to 10) phase with a lower oxidation state of Ti. The second-step weight loss is mainly attributed to the conversion of T_nO_{2n-1} to TiC_xO_y [25]. Moreover, the final weight loss is governed by the continuous formation of TiC from a non-stoichiometric TiC_xO_y phase. The overall weight loss during this pyrolysis process was observed to be 47.89%, which agrees with the theoretical reduction of TiO_2 to TiC. Hence, the entire pyrolysis procedure can be described by the above-mentioned three-step process, and the carbothermal reduction of TiO_2 completes at approximately 1378 °C. This is possible because of the fact that the formation of CO is almost complete in the aforementioned dynamical conditions. In a recent article, it was observed that the reduction of TiO_2 to TiC is promoted via the formation of various suboxides at different temperatures[20]. However, in that work, the intermediate suboxide peak at 1050 ^{o}C was not observed. This indicates a rapid and direct conversion of TiO_2 to TiC_xO_y. Such variation in transformation temperature is due to the starting precursor particle size and reaction atmosphere. In our study, the powder processing temperature was lower compared to that of the dynamic pyrolysis behavior. This difference in temperature appears to be beneficial for the synthesis of ceramic nano particles[26].

XRD pattern indicates the precursor TiO_2 nano particles to be entirely composed of the low crystalline rutile phase and the as-synthesis pure TiC crystalline phase without the presence of any TiO_2 or intermediate phases (Fig. 3). The Pawley refinement result shows that the synthesized nano TiC particles are of cubic symmetry with Fm-3m space group having Z = 4 and lattice parameters a = b = c = 4.3049(6) ´. The inset XRD pattern of the powders calcined at 1200 ^{o}C exhibits low angle shift, which indicates an increment in lattice spacing due to the

presence of oxygen ions. In other words, the TiO_2 and carbon powder mixture forms a TiC_xO_y phase at low temperature. XRF confirmed that the Ti:C:O ratio at the intermediate stage was 1:0.68:0.32, whereas the as-synthesis TiC powder calcination at 1350 ^oC for 1 hour is free from any element or impurity.

High temperature synthesis induces strain in nano particles; therefore, an estimation of strain is important. The Williamson–Hall method was employed to calculate the volume weighted crystallite size as well as the residual strain of the synthesized TiC nanoparticles[22]. The process of determining particle size and strain from the obtained slope is illustrated in Fig. 4, where Y represents $b \cos \theta$, and X represents $2 \sin \theta$. Hence, the slope represents the strain (η), and the volume weighted crystallite size was calculated from the intercept (λ/d). The average crystallite size and strain of nano TiC particles was calculated as 91 nm and 0.2%, respectively. The strain of the particle reduced to 0.07% and its morphology tended to near-equilibrium shape with increasing time up to 4 hours. In a recent article, the strain of 107 nm sized TiC nano particles was reported to be 0.61% [18].

In the present case, the volume weighted crystallite size, obtained from XRD analysis, was further confirmed by TEM analysis. The changes in particle morphology after synthesizing for different lengths of time were also investigated using TEM. Typical TEM images of TiC particles synthesized at 1350 ^oC for 1, 2, and 4 hours are shown in Figs. 5a-c, 5d-e and 5f-g, respectively. The lattice parameter obtained for 1 hour calcination matches well with that obtained from the XRD analysis. The particles synthesized at 1350 ^oC for 1 hour are nearly spherical; however, particle size increases with time. The development of faceted grain morphology with sizes up to 200 nm was noticed for longer thermal treatments. The anisotropic grain growth possibly reduces the strain in TiC particles, as reported in Table 1.

A detailed investigation of particle size distribution is helpful in predicting the consolidation behavior of nanopowders. We emphasize that agglomeration during compaction,

which leads to interparticle and interagglomerate pores, is a critical problem and leads to inhomogeneous densification of the compact. For nanopowders, interagglomerate pores are typically larger than interparticle pores. In general, commercially available ceramic powders are designated by their *mean* particle size, for example 100 nm, 500 nm, 1 μm etc, without mentioning particle size *distributions*. Here, we address this deficiency using a mathematical approach. Usually, the normal distribution represents the average particle size (D_{50}); however, we employed Weibull analysis, which demonstrates the maximum appearance of the particles in sizes, when compared to normal distribution ($D_{63}>D_{50}$). Recently, Ramakrishnan studied the particle size distribution of different ceramic particles, such as TiO_2 and ZrO_2, through the two-parameter Weibull distribution[27]. However, the degree of distribution (α) or maximum appearance of particles in size (β) has not been studied. Thus, it is difficult to understand the real meaning of the size distribution without representative data for the distribution parameters. We selected a three-parameter Weibull distribution function that includes a correction parameter in order to model particle size distributions obtained from SMPS measurements[28] (Fig. 6a):

$$f(x) = 1 - \exp\left[-\left(\frac{x-\gamma}{\beta}\right)^{\alpha}\right] \quad \cdots\cdots\cdots\cdots\cdots\cdots (2)$$

Here, x, α, β, and γ are all positive, and $f(x)$ is the cumulative undersize percent of particle size x present in the distribution. Three parameters α, β, and γ represent shape, scale, and location, respectively. The values of these parameters can be obtained using linear fits between ln ln[1/(1-$f(x)$)] and Ln(x-γ) (Fig. 6b). In the present case, we are able to achieve good fits to the SMPS data using the above three-parameter distribution function using α, β, and γ equal to 0.96, 84, and 11, respectively. The shape parameter for the synthesized TiC nano particles represents smaller value, indicating wider size distribution. The scale parameter indicates that most particles are 84 nm in size, and the location parameter indicates the minimum particle size to be 11 nm.

The as-realized wide distribution is presumably due to the presence of nano particles in water and partial formation of agglomerates during SMPS analysis. The as-obtained β value from the Weibull analysis gradually increases with increasing reaction time, which was also confirmed through TEM analysis. Table 1 represents the physical properties of as-synthesized TiC nanoparticles at 1350 ^{o}C. The shape parameter (α) indicates a wider distribution, which is presumably due to the coarsening effect with increasing time. Based on the Weibull analysis, the size parameters were fitted with a power-law ($d^n - d^n_o = At$, where, d_o particle diameter at initial time '*t*' in min, *A* = constant) of particle coarsening. The calculated coarsening exponent (n) for the presently described synthesis process is found to be 2.9 ($3 > n > 2$), which agrees with previous grain growth study[29,30]. Volume diffusion is the probable growth mechanism for this process.

4. Conclusions

Based on the present work, the following conclusions can be drawn:

a) The present work demonstrates that carbothermal reduction of nanosized rutile with amorphous carbon at a (relatively) low temperature of 1350 ^{o}C for 1 hour leads to the nanosize pure TiC particles. Longer holding times leads to the well-faceted TiC particle.

b) The synthesis mechanism has been described by a three-stage process of reduction of TiO_2 to TiC phase: first, formation of an unstable oxygen deficient T_nO_{2n-1} phase; second, conversion of T_nO_{2n-1} to TiC_xO_y; and third, formation of TiC from non-stoichiometric TiC_xO_y phase.

c) The as-synthesized TiC nanoparticles are nearly spherical with sizes below 100 nm and compositionally pure. Such particles can be synthesized at relatively low temperatures.

d) The three-parameter Weibull function is useful for describing the particle size distribution and their magnitudes. Experiments carried out at varying synthesis time of at 1350 ^{o}C revealed the coarsening behavior and the particle coarsening exponent (n) to be 2.9. Additionally, the particle shape changed from spherical (1 hour) to more faceted for longer holding times of 4 hours.

References

1. A. Mukhopadhyay and B. Basu, "Consolidation-Microstructure-Property relationships in Bulk Nanoceramics and Ceramic Nanocomposites: A review**,"** International Materials Reviews. **52** [5] 257-288 (2007).
2. E.K. Stroms, "The Refractory Carbides, Refractory Materials Series," *Academic Press, New York,* 2 (1967).
3. L.E. Toth, "Transition Metal Carbides and Nitrides*" Academic Press, New York,* (1971).
4. R. Koc and J.S. Folmer, "Carbothermal synthesis of titanium carbide using ultrafine titania powders," *J. Mater. Sci.* **32** [12] 3101-3111 (1997).
5. N.A. Hassine, J.G.P. Binner and T.E. Cross, "Synthesis of Refractory Metal Carbide Microwave Carbothermal Reduction*," Int. J. Refract. Met. Hard Mater.* **13** [6] 353-358 (1995).
6. H. Preiss, L.M. Berger and D. Schultze, "Studies on the Carbothermal Preparation of Titanium Carbide from Different Gel Precursors," *J Eur Ceram Soc.* **19** [2] 195-206 (1999).
7. Z. Jiang and W.E. Rhine, **"**Preparation of titanium nitride (TiN) and titanium carbide (TiC) from a polymeric precursor," *Chem. Mater.* **3**, 1132-1137 (1991).
8. S. Dutremez, P. Gerbier, C. Guerin, B. Henner and P. Merle, "Metal Alkoxide/Hexa-2,4-diyne-1,6-diol Hybrid Polymers: Synthesis and Use as Precursors to Metal Carbides and Nitrides," *Adv. Mater.* **10**, 465-470 (1998).
9. D.B. Miracle and H.A. Lipsitt, "Mechanical Properties of Fine-Grained Substoichiomebic Titanium Carbide," *J. Am. Ceram. Soc.,* **66** [8] 592-597 (1983).
10. H.O. Pierson, "Handbook of Refractory Carbides and Nitrides," *Noyes Publications, Westwood.* (1996).

11. H.H. Nersisyan, J.H. Lee, C.W. Won, "Self-propagating high-temperature synthesis of nano-sized titanium carbide powder," *J. Mater. Res.* **17** [11] 2859-64 (2002).
12. D.W. Lee and B.K. Kim, "Synthesis of nano-structured titanium carbide by Mg-thermal reduction*" Scr. Mater.* **48** [11] **1513**-1518 (2003).
13. R. Alexandrescu, E. Borsella, S. Botti, M.C. Cesile, S. Martelli, R. Giorgi, S. Turtŭ, G. Zappa, "Synthesis of TiC and SiC/TiC nanocrystalline powders by gas-phase laser-induced reaction," *J. Mater. Sci.* **32** [11] 5629-5635 (1997).
14. X.L. Cui, L.S. Cui, L. Wang and M. Qi, "Synthesis of titanium carbide powder from TiO_2 and petroleum coke by reactive milling," *Petrol. Sci. Technol.* **20,** 999-1007 (2002).
15. M. S. Noel and D. Kovar, "Laser chemical vapor deposition of TiC on tantalum,"*J. Mater. Sci.* **37** [4]**,** 689-697 (2002).
16. N. J. Welham and D. J. Llewellyn, "Formation of Nanometric Hard Materials by Cold Milling," *J. Eur. Ceram Soc.* **19** [16]**,** 2833-41 **(**1999).
17. Y-C. Woo, H-J. Kang and D. J. Kim, "Formation of TiC particle during carbothermal reduction of TiO2," *J. Eur. Ceram. Soc.* **27** [2-3], 719-722 (2007).
18. M. Razavi, M.R. Rahimipour and R. Mansoori, "Synthesis of $TiC–Al_2O_3$ nanocomposite powder from impure Ti chips, Al and carbon black by mechanical alloying,," *J. Alloys and Compounds,* **450** [1-2] 463-467 (2008).
19. X. Fenga, Y. Baia, B. Lub, C-G. Wanga, Y.X. Liua, G.L. Genga and Li Lic, "Easy synthesis of TiC nanocrystallite*," J. Cryst. Growth* **264** [1-3] 316-319 (2004).
20. Y. Gotoh, K. Fujimura, M. Koike, Y. Ohkoshi, M. Nagura, K. Akamatsu, S. Deki, "Synthesis of titanium carbide from a composite of TiO_2 nanoparticles/methyl cellulose by carbothermal reduction," *Mat. Res Bull.* **36** [13-14] 2263-2275 (2001).
21. D. Sarkar, M. C. Chu, S. J. Cho and K. Y. Yoon, "Barium Titanate Nanoparticles and Method of Preparing the Same," *Korean-Patent,* **10-2007-0119498** (2007).

22. G.K. Williamson and W.H. Hall, "X-ray line broadening from filed aluminium and wolfram,"*Acta Metall.*, **1** [1], 22-31 (1953).

23. Y. Chen, A. Lin and F. Gan, "Preparation of nano-TiO_2 from $TiCl_4$ by dialysis hydrolysis," *Powder Tech* **167** [3]**,** 106-109 (2006).

24. M. Ramanoorthy and D. Vanderbilt, R. D. King-Smith, "First-principles calculations of the energetics of stoichiometric TiO_2 surfaces,"*Phys. Rev. B* **49** [23]**,** 16721-27 (1994).

25. G. V. White, K. J. D. Mackenzie, I. W. M. Brown, M. E. Bowden and J. H. Johnston, "Carbothermal synthesis of titanium nitride," *J. Mat. Sc.*, **27** [16]**,** 4294-99 (1992).

26. D. Sarkar, D. Mohapatra, S. Ray, S. Adak and N.K. Mitra, "Synthesis and Characterization of Zirconia doped Alumina Nanopowder," *Ceram Inter.*, **33** [7] 1275–1282 (2007).

27. K.N. Ramakrishnan, "Powder particle size relationship in microwave synthesized ceramic powders,"*Mat. Sc. and Engg.*, **A259** [1]**,** 120-125 (1999).

28. G.J. Hahn and S.S. Shapiro, "Statistical Models in Engineering," *Wiley, New York*, (1967), p.287.

29. L. Huimin, HE Jianping, Y Bin, Z Jishan, "Grain growth law of semi-solid state TiC_p/7075 Al alloy prepared by spray deposition," *Acta Meta Sinica,* **42** [2] 158-162 (2006).

30. G. C. Nicholson, "Grain Growth in Magnesium Oxide Containing a Liquid Phase," *J. Am. Ceram. Soc.*, **48** [10] 525-528 (1965)

Table Captions:

Table 1: Physical properties of TiC nanopowders synthesized at 1350^{o}C for varying timescale.

Figure Captions:

Figure 1: TEM image of synthesized needle-like rutile (TiO_2) particles (a), and 5 nm oval-shaped primary particles adhering through head-to-tail arrangement and form agglomeration (b).

Figure 2: Non-isothermal DTA-TG analysis of TiO_2 and carbon black mixture in Ar atmosphere at a heating rate of 10^{o}C/min. An endothermic peak is observed at 1114^{o}C. The TG curve is linear beyond 1378^{o}C and resultant weight loss is 47.89%.

Figure 3: XRD patterns of the synthesized TiC phase at 1350^{o}C for 1 hour. Inset indicates the presence of rutile phase in precursor TiO_2 and peak shifting (at 1200^{o}C) due to non-stoichiometric TiC_xO_y phase.

Figure 4: TiC nano particle size and strain measurements after synthesis at 1350^{o}C for 1 hour. The particle size (b = 91.15 nm) and strain (slope(η) = 0.00206) was calculated using the Williamson–Hall equation.

Figure 5: TEM analysis of the TiC phase synthesized at 1350^{o}C for 1 hour (a-c), 2hour (d-e) and 4 hours (f-g), respectively. The particles are more faceted and that average particle size increases with processing time.

Figure 6: Particle Size Distribution of TiC nano powders synthesized at 1350^{o}C for 1 hour (a) and three-parameter Weibull distribution plot, where α and β represents the shape and the scale parameters, respectively; calculated from linear fit of SMPS data (b).

List of Tables:

Table 1:

Processing Time (hr)	Strain (%)	Morphology	Weibull Parameters (size distribution)	
			Shape (α)	Scale (β)
1	0.20	Spherical	0.9582	84
2	0.12	Near Spherical	0.9372	117
4	0.07	Faceted	0.9254	162

List of Figures:

Fig 1:

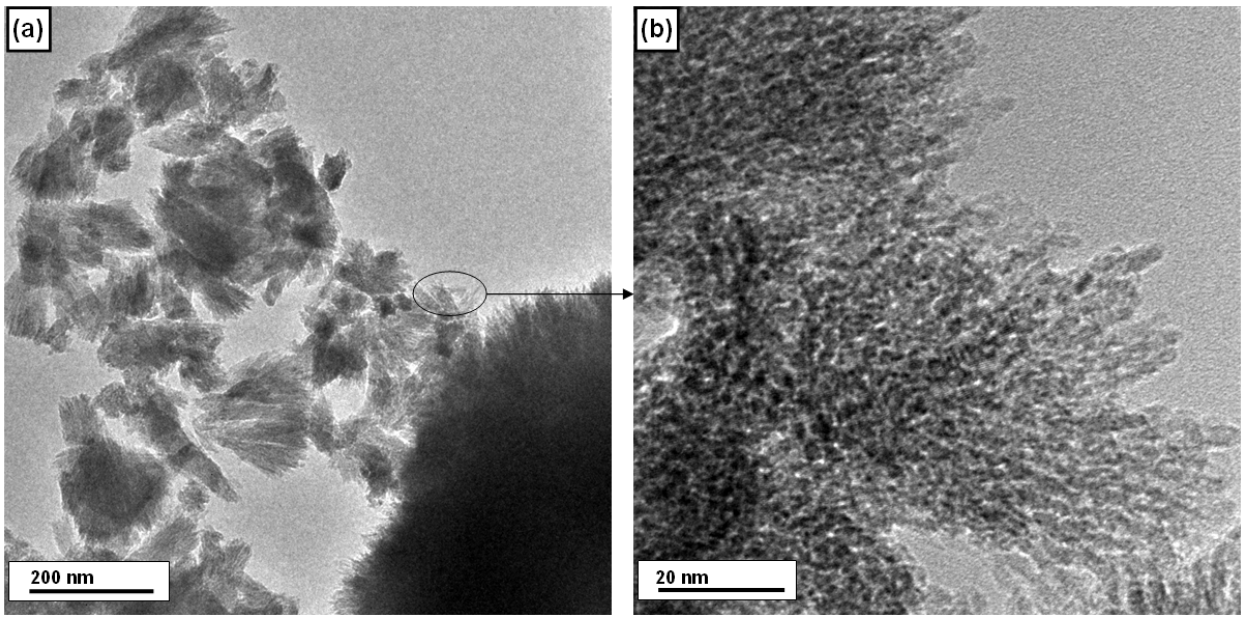

Fig 2:

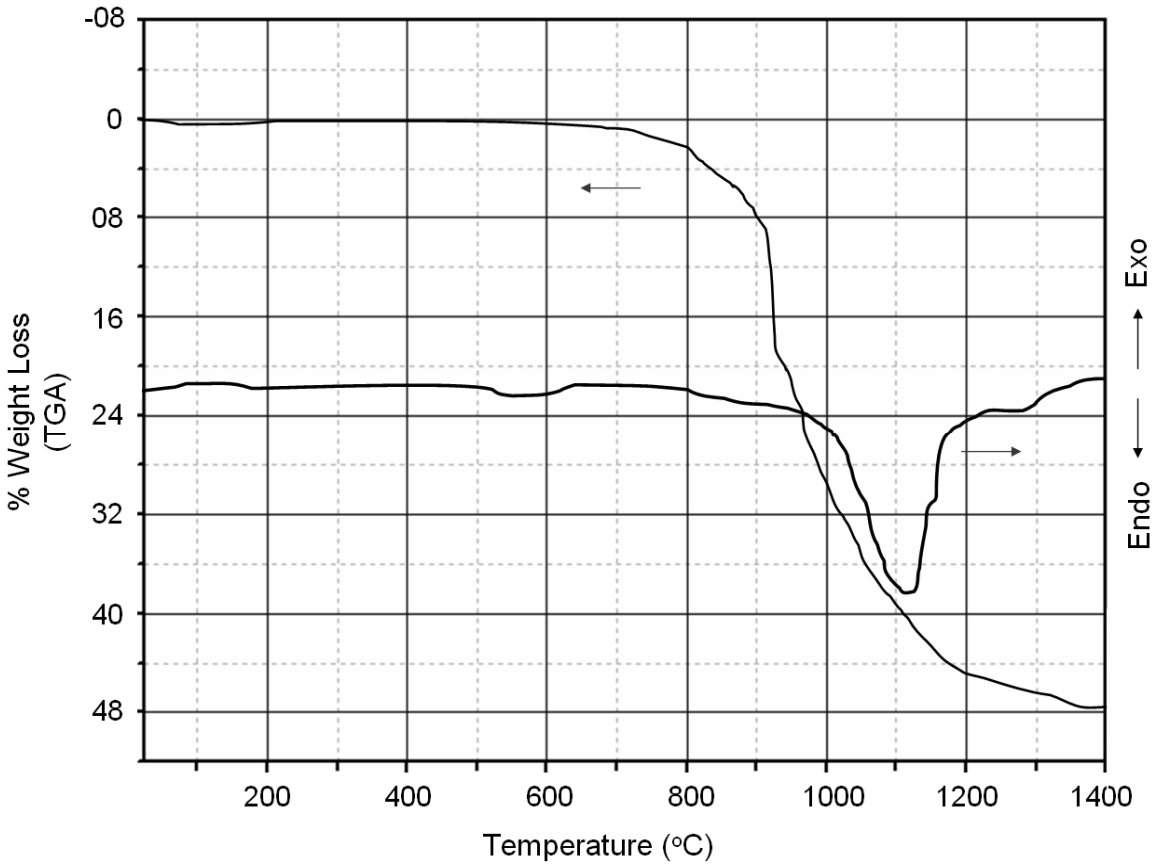

Fig 3:

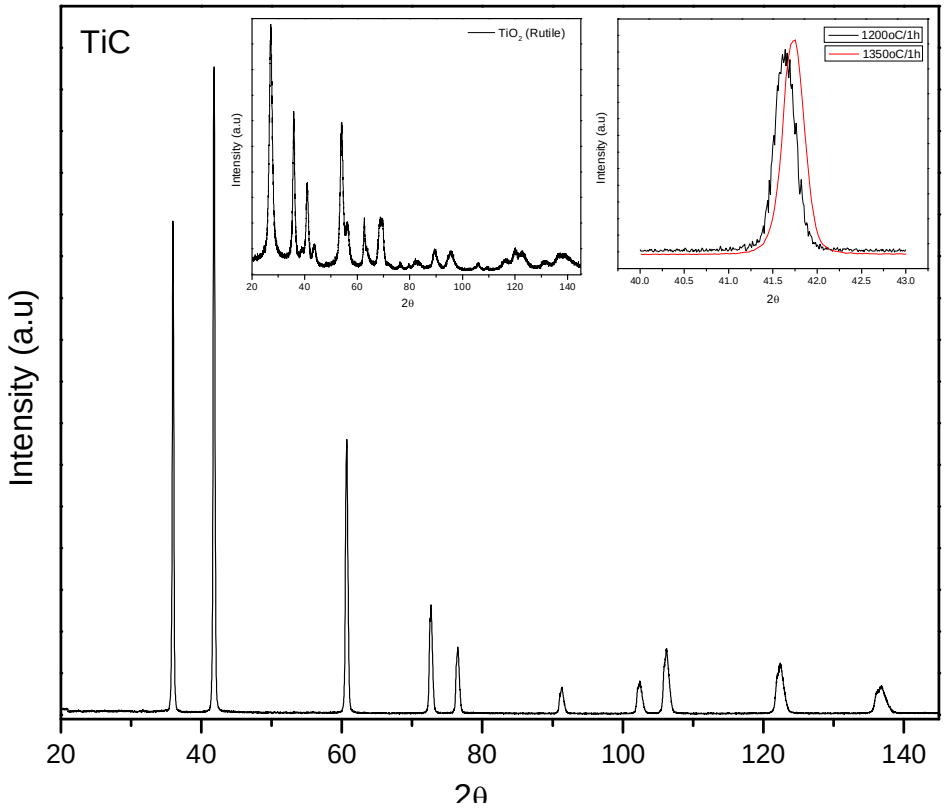
TiC
TiO2 (Rutile)
Intensity (a.u)
2θ
1200oC/1h
1350oC/1h
Intensity (a.u)
2θ
Intensity (a.u)
20
40
60
80
100
120
140
2θ

Fig 4

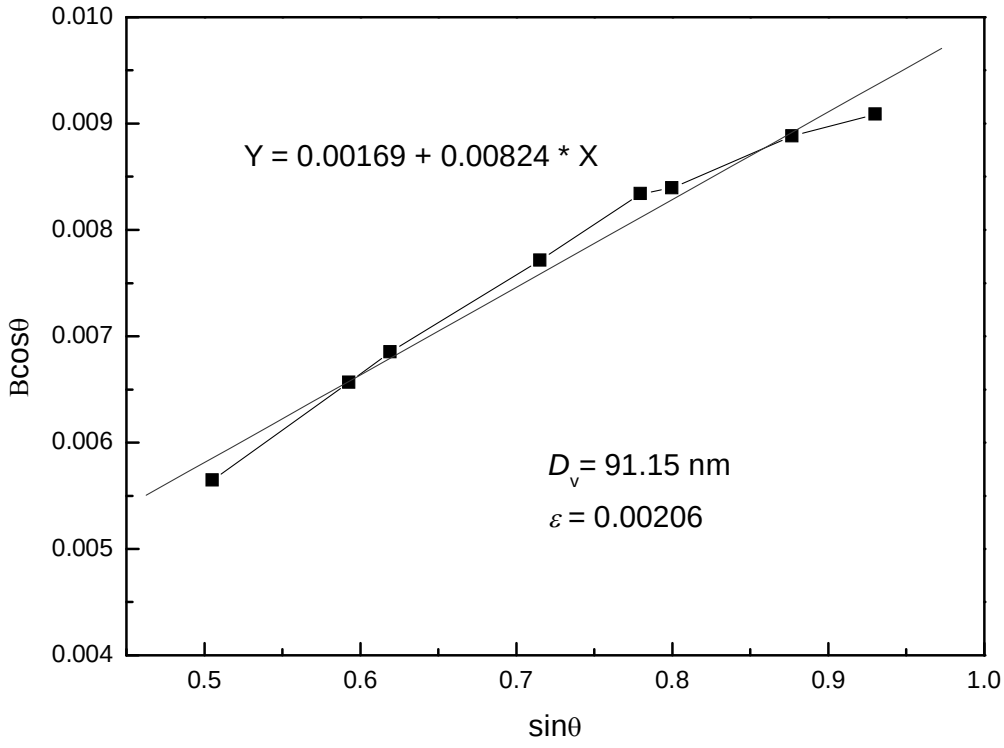
Y = 0.00169 + 0.00824 * X
D_v = 91.15 nm
ε = 0.00206
Bcosθ
sinθ
0.010
0.009
0.008
0.007
0.006
0.005
0.004
0.5
0.6
0.7
0.8
0.9
1.0

Fig 5:

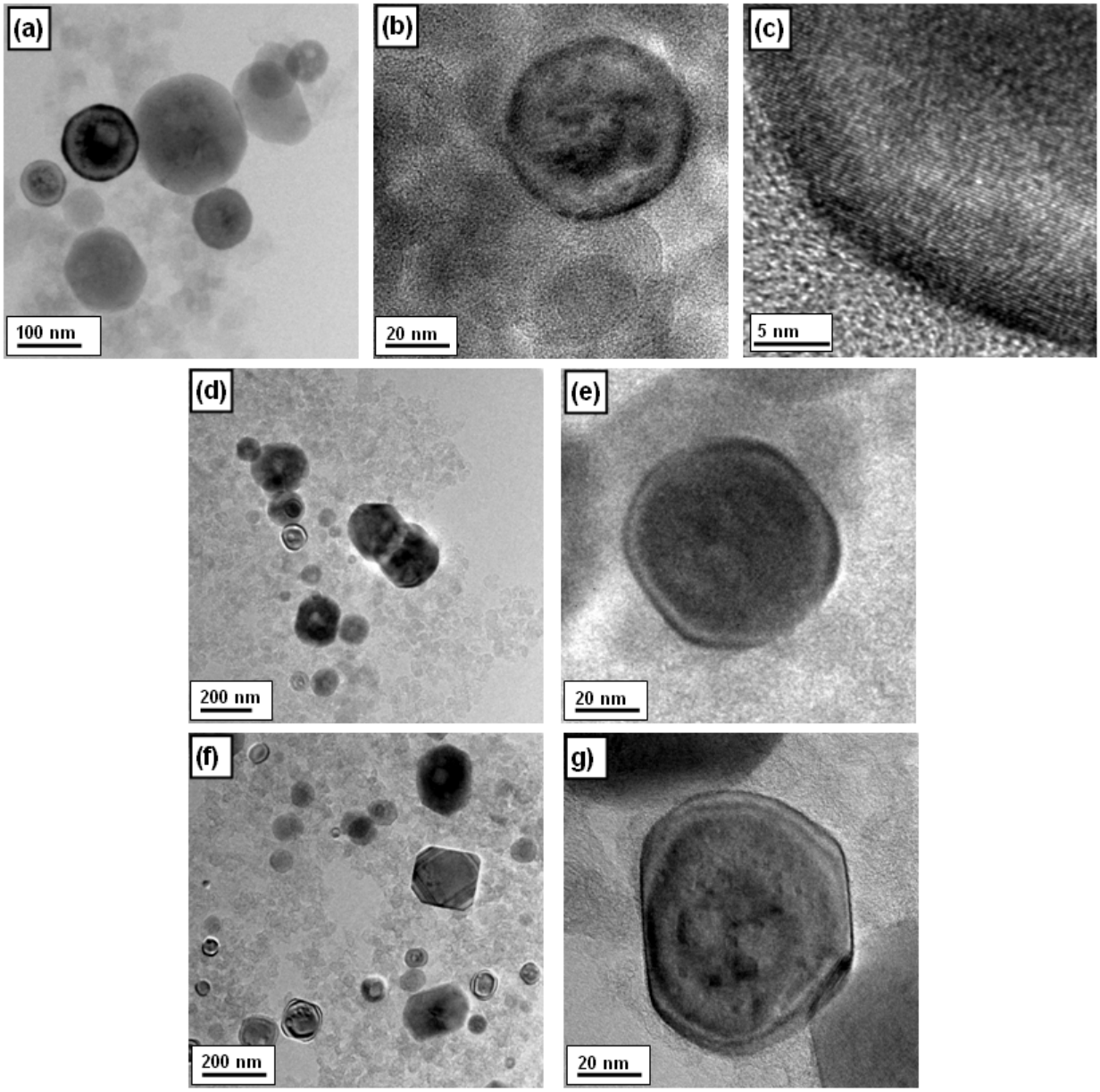

Fig 6:

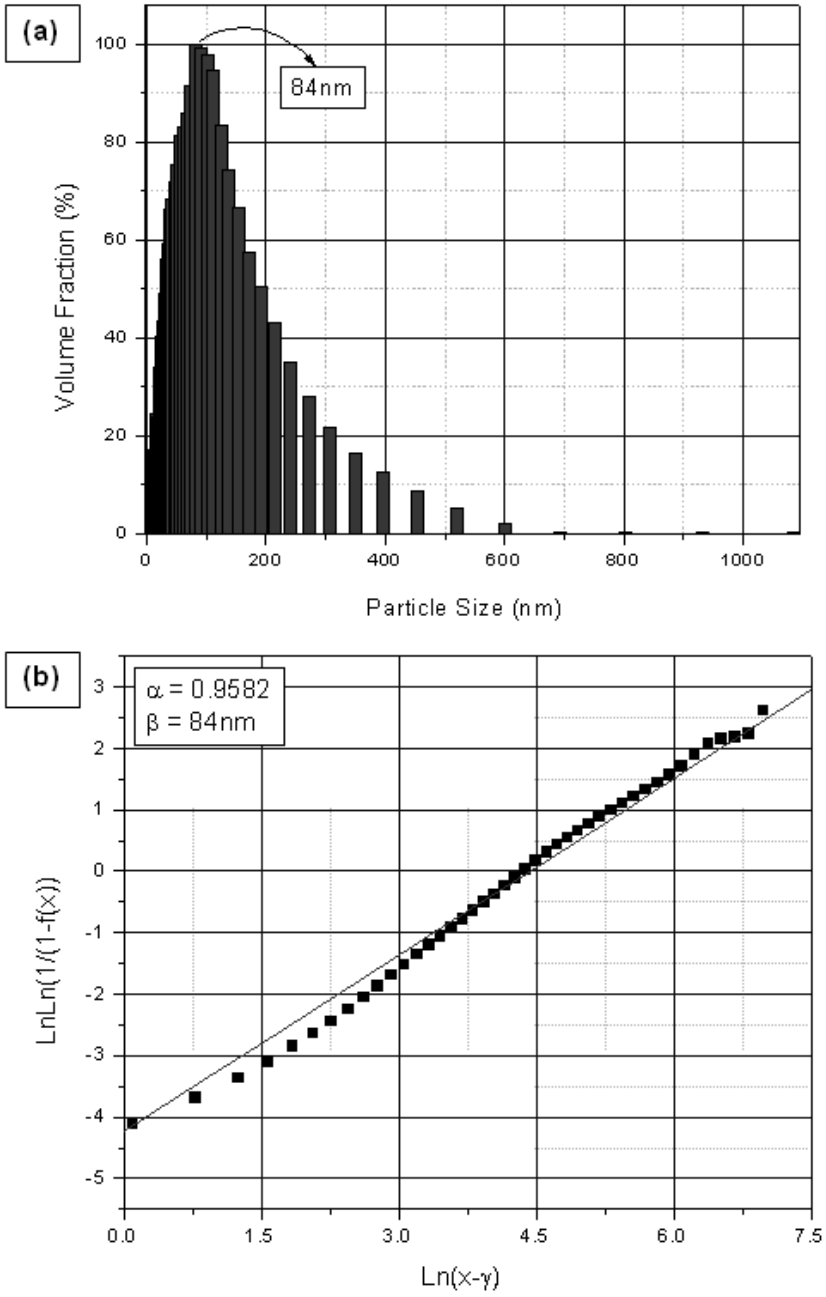
(a)
84nm
Volume Fraction (%)
Particle Size (nm)
(b)
α = 0.9582
β = 84nm
LnLn(1/(1-f(x)))
Ln(x-γ)